

Proceedings of the Korean Nuclear Society Spring Meeting  
Kwangju, Korea, May 1997

## ICRF Wave Propagation and Absorption on KSTAR Plasma

M.H. Ju, B.G. Hong and J.M. Han  
T. K. Mau\*

Korea Atomic Energy Research Institute  
\*University of California at San Diego, San Diego, California

### Abstract

For the efficient current drive, the structure of ICRF wave propagation and absorption in a tokamak plasma should be first investigated. In this paper, two dimensional study on FWCD as well as ICRF minority ion heating for the KSTAR [Korea Superconducting Tokamak Research] [1] plasma was performed using the full wave code of TORIC [2]. The ICRF wave propagation and absorption structures, the competitive power absorption between electrons and ions and the coupling of antenna/plasma are investigated.

### I. Introduction

One of the KSTAR research objectives is to explore the methods to achieve the steady state operation for tokamak fusion reactors using non-inductive current drive. Heating and current drive with ICRF fast waves are one of the main features in the operation of the reversed shear plasma on KSTAR. Numerical investigations of the ICRF wave propagation and absorption are performed using the global wave code, TORIC. The code TORIC solves the finite Larmor radius wave equations in the ion cyclotron frequency range in an arbitrary axisymmetric toroidal geometry. Table 1 describes the reference KSTAR plasma and antenna parameters. With  $B_0=3.5$  T, the baseline heating scenario is to use the minority heating

Major Radius $R_o$	1.8 m
Minor Radius $a$	0.5 m
Toroidal Field $B_o$	3.5 T
Plasma Current $I_p$	2.0 MA
Elongation $\kappa$	2.0
Triangularity $\delta$	0.8
Antenna Radius	54.5 cm
Faraday Shield Radius	52.0 cm
Poloidal Length	70.0 cm

Table 1: The Reference KSTAR Parameters

of  $H^+$  in H/D plasma (H:5% and D:95%). Considering the Shafranov shift of magnetic axis,  $\omega=51$  MHz is set for ICRF heating. For FWCD, we use the frequency of 38 MHz to remove all ion cyclotron resonance surfaces from the plasma. The density and temperature profiles are assumed to be parabolic with the exponential decay at the edge:  $n_e(0)=1 \times 10^{14}/cm^3$ ,  $n_e(sep) = 0.25 \times n_e(0)$ , density decay length=2cm,  $T_e(0)=T_H(0)=T_D(0)=10$  keV,  $T_e(sep)=0.25 \times T_e(0)$ , temperature decay length=5cm. In all calculations presented, the numbers of poloidal modes and radial grids are set to 31 and 301, respectively. These numbers resulted in the relatively good convergence within a few % for a typical range of the toroidal mode number.

## II. Minority Heating of $H^+$ in a $D^+$ Plasma

Figure 1 displays the flux-surface averaged power deposition profiles of plasma species for  $T_e(0)=10$  keV (Fig. 1 (a)) and  $T_e(0)=2$  keV (Fig. 1 (b)) when  $n_\phi=20$ . In the high temperature case, the wave damping on the electrons is more dominant than on the ions:  $P_H=13.6\%$ ,  $P_D=1.9\%$ ,  $P_e=84.3\%$ ,  $P_{IBW}=0.1\%$ . This abnormal electron dominant heating phenomenon is attributed to the variation of  $k_{\parallel}$  by the strong B poloidal magnetic field effect at the high temperature. With  $T_e(0)=2$  keV, the ions absorb more power through fundamental ion cyclotron resonance:  $P_H=74.0\%$ ,  $P_D=3.3\%$ ,  $P_e=21.1\%$ ,  $P_{IBW}=1.3\%$ . In figure 2, the contour plots of fast wave com-

$T_{e0}$ (keV)	$n_{e0}$ ( $10 \times 10^{14} \text{ cm}^{-3}$ )	$n_\varphi$	$I/P$ (A/W)	$\gamma_{CD}$
10.	1.0	5	0.031	0.024
10.	1.0	10	0.038	0.039
10.	1.0	15	0.051	0.039
12.5	0.8	10	0.068	0.042
15.	0.67	10	0.089	0.046

Table 2: Current Drive Results for KSTAR

ponent ( $E_-$ ) in the poloidal cross section for  $T_e(0)=10$  keV (Fig. 2 (a)) and  $T_e(0)=2$  keV (Fig. 2 (b)) are shown for  $n_\varphi=20$ . The fast wave excited from the low field side antenna propagate towards the magnetic axis, on which the wave energy is damped on the plasma electrons and ions through the resonances. Some part of fast wave penetrate also towards the high field side and then is mode-converted to the ion Bernstein wave. It is noted that the high temperature case indicates the stronger damping of the fast wave energy on the magnetic axis while the lower temperature case shows the stronger mode conversion to IBW in the high field side.

### III. Fast Wave Current Drive

In this case, the electrons absorb over 90% of total input power through TTMP. In figure 3 (a), the contour plot of fast wave component ( $E_-$ ) in the poloidal cross section is shown for  $n_\varphi=20$ . Figure 3 (b) shows the loading resistance (ohm) spectrum scanned over the toroidal modes ( $0 < n_\varphi < 36$ ) for  $T_e(0)=10$  keV and 2 keV. Compared to the high temperature, the lower temperature case shows some structure in the loading resistance spectrum. However, the value of loading resistance itself for each  $n_\varphi$  mode was similar in both cases except the lower  $n_\varphi$  modes of  $< 10$ . We have incorporated the capability of calculating the driven current density due to electron absorption of fast wave power into TORIC, using a standard model. The local driven current density,  $j_{||}(\psi, \vartheta)$ , can be related to the local electron power absorption,  $p_e(\psi, \vartheta)$  by

$$j_{||}(\psi, \vartheta) = \eta_{CD}(\psi, \vartheta, k_{||})p_e(\psi, \vartheta) \quad (1)$$

where  $\eta_{CD}(\psi, \vartheta, k_{\parallel})$  is the normalized current drive efficiency [3]. Our preliminary analysis shows that the driven current density profiles due to the ICRF fast waves follow those of the absorption profiles, as expected. As an example, the results for the standard KSTAR case ( $f = 38$  MHz,  $T_{e0} = 10$  keV,  $n_{e0} = 1 \times 10^{14}$  cm $^{-3}$ ,  $n_{\varphi} = 10$ ) are shown in Fig. 4 (a) and (b), where the absorption and driven current profiles are displayed. In Table 2, we show the results of several cases for various values of  $n_{\varphi}$  and  $T_{e0}$  at fixed  $\beta$ . The normalized current drive efficiency,  $\gamma_{CD} \equiv \bar{n}_e [10 \times 10^{14} \text{ cm}^{-3}] I_{CD} [MA] R [m] / P_{CD} [MW]$ , has been shown to increase with temperature at fixed  $\beta$ .

### Acknowledgement

The authors wish to thank Dr M. Brambilla of Max-Planck-Institut for his useful discussion.

### References

- [1] G. S. Lee et al. Bulletin of the American Physical Society, Vol 41, No. 7, p1439,1996.
- [2] M. Brambilla, "A Full Wave Code for Ion Cyclotron Waves in Toroidal Plasma," Report IPP 5/66, Garching (1996).
- [3] D. A. Ehst, C. F. F. Karney, *Nucl. Fusion* **31** (1991) 1933.

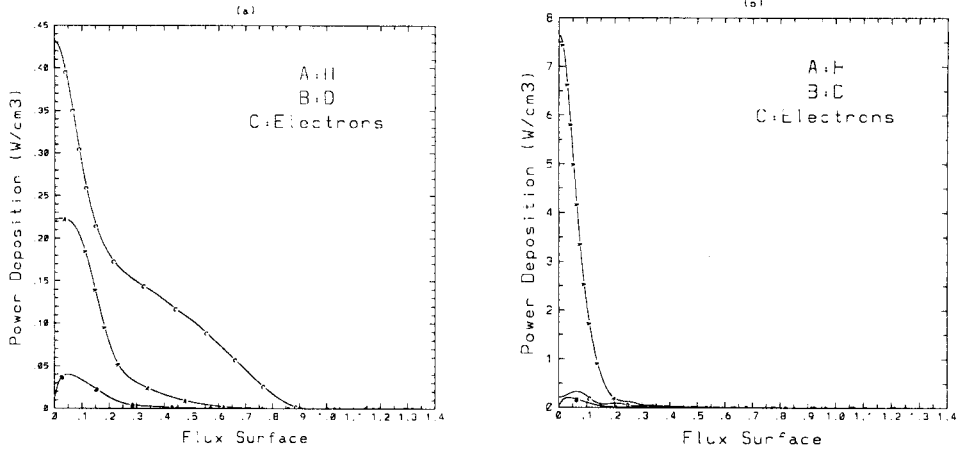


Figure 1: Flux-Surface Averaged Power Deposition Profile (a) at  $T_e(0)=10$  keV and (b) at  $T_e(0)=2$  keV for Minority Heating of  $H^+$  in a  $D^+$  Plasma

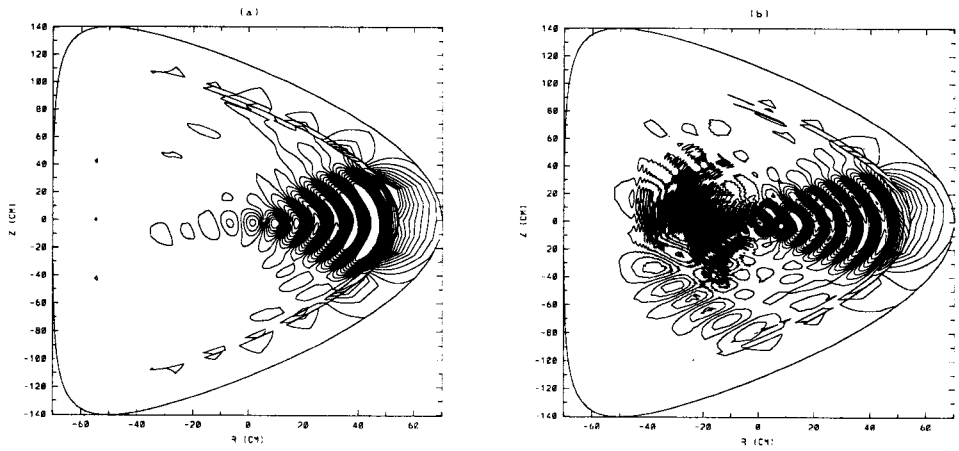


Figure 2: Contour Plots of Fast Wave Component ( $E_-$ ) in Poloidal Cross Section (a) at  $T_e(0)=10$  keV and (b) at  $T_e(0)=2$  keV for Minority Heating of  $H^+$  in a  $D^+$  Plasma

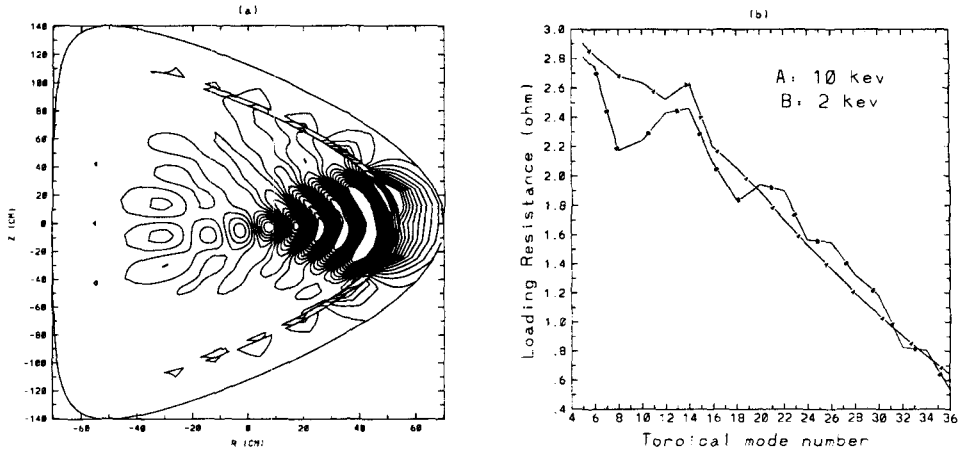


Figure 3: (a) Contour Plot of Fast Wave Component ( $E_-$ ) in the Poloidal Cross Section and (b) Loading Resistance (ohm) Spectrum Scanned over the Toroidal Mode Numbers ( $0 < n_\varphi < 36$ ) for  $T_e(0) = 10$  keV and 2 keV for Fast Wave Current Drive

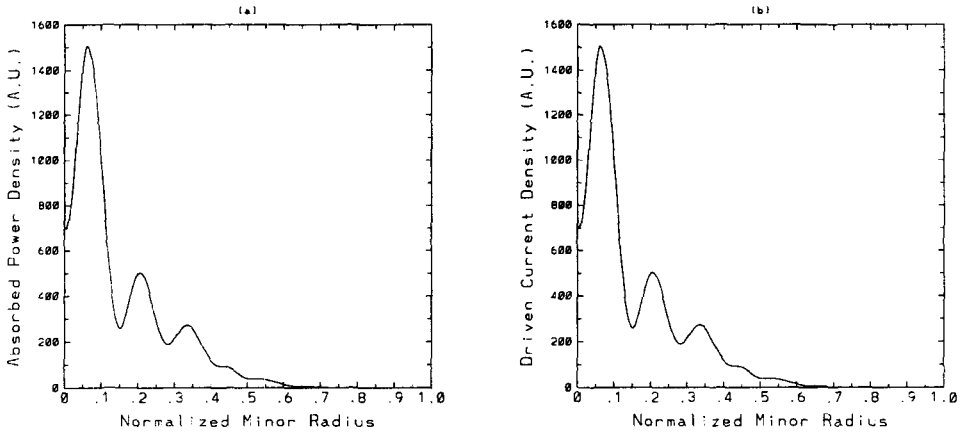


Figure 4: (a) Radial Profile of Electron Absorption of Fast Wave Power and (b) Radial Profile of Fast Wave Driven Current Density for KSTAR Reference Case for Fast Wave Current Drive